PERFORMANCE OF LAMINAR-FLOW LEADING-EDGE TEST ARTICLES IN CLOUD ENCOUNTERS

Richard E. Davis, Dal V. Maddalon, and Richard D. Wagner
NASA Langley Research Center
Hampton, Virginia

[redacted]

BACKGROUND

MECHANISM FOR LOSS OF LAMINAR FLOW IN PARTICLES

The problem of cloud effects on LFC* aircraft was first noticed on the USAF X-21 program when, during flight testing at typical cruise conditions of M = 0.75 and 40,000 ft. altitude, it was observed that laminar flow was totally lost whenever the aircraft penetrated cirrus clouds, with horizontal visibilities estimated to be about 5,000-10,000 feet. Also, LFC performance was observed (ref. 1) to be partially degraded or erratic when penetrating light cirrus haze, even when the horizontal visibility was as much as 50 miles. (As will be described later in this paper, cirrus clouds, both thick and tenuous, are causing similar corresponding effects on the LEFT+ JetStar aircraft). At these altitudes, cirrus clouds are composed mainly of ice crystals. These crystals have a detrimental effect on maintaining laminar flow, depending on their size and concentration (or flux as perceived by the aircraft). To explain the erratic LFC performance on the X-21, Hall (ref. 2) developed a theory to predict the effect of ice particle encounter on the maintenance of laminar flow. The theory postulated that ice particles entering the laminar boundary layer shed turbulent vortices; these vortices cause transition in the main flow (Fig. 1). As shown on the figure, the key factors which determine whether any given cloud encounter will cause total, partial, or negligible loss of laminar flow are the particle size, the particle concentration, and the particle's residence time in the boundary layer. Pfenninger (ref. 3) has suggested that wing sweep is also a key factor.The spanwise flow on a swept wing can lead to greater particle wake velocity defects, which promote increased turbulence production, and the increased effective chord results in higher particle residence time in the boundary layer.

*Laminar-flow control (LFC)
+Leading-Edge Flight Test (LEFT)

ICE PARTICLE DEGRADATION OF LAMINAR FLOW

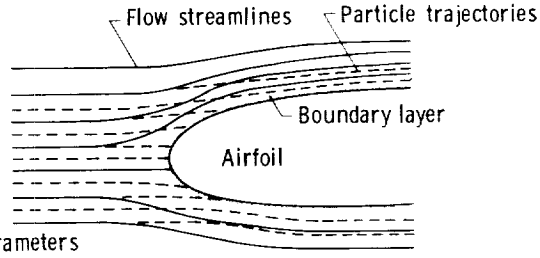

Key parameters

- Particle size
- Particle flux or concentration
- Particle duration in boundary layer
- Particle Reynolds Number
- Airfoil L.E. geometry
- Wing sweep

Mechanism for laminar flow loss

- Some particles enter laminar boundary layer
- Wakes shed from particles become turbulent and trigger boundary-layer transition

Figure 1

BACKGROUND

HALL CRITERIA FOR LOSS OF LAMINAR FLOW ON X-21

Hall's theoretical analysis considered only columnar ice crystals of length-to-diameter ratio 2.5, because that crystal form was assumed to be the predominant one. When the theoretical impingement dynamics of this type of particle on an elliptical approximation of the forward portion of the X-21 airfoil were considered, the results indicated that, for M = 0.75 and 40,000 ft. altitude, particles smaller than 4 micrometers (μm) in length will not impinge on the airfoil surface, but particles larger than about 50 μm will impinge at near free-stream velocity. If the particles are very small, i.e. shorter than 4 μm, aerodynamic forces predominate over inertia forces and most particles follow streamlines and few enter the boundary layer. As the ice particles become larger in size, they begin to penetrate the laminar boundary layer but do not cause a breakdown to turbulent flow until some critical size is attained. However, particles of this critical size must be present in a sufficiently large concentration in order to cause boundary-layer transition. Figure 2, from Hall's analysis, illustrates the above discussion for flight conditions of M = 0.75 and 40,000 ft. altitude. It should be noted that equivalent melted diameter, EMD, is chosen as the abscissa variable on the figure. It has been found that ice particles in cirrus clouds occur in several crystalline forms, and that the columnar variety is not necessarily the most numerous. (In any event, the regions on the figure pertain to columnar crystals). According to the analysis, for columnar ice particles with an EMD of less than 33 μm EMD, particle concentrations smaller than about 500 particles/m^3 produce no effect on maintaining laminar flow (LF)[region 2 of the figure]. As particle concentrations increase above about 500 particles/m^3 (for EMD greater than 33 μm), there is an increasingly detrimental effect on laminar flow (regions 3 and 4 of the figure).

It should be emphasized that the critical values of ice-particle size and concentration level depicted in Figure 2 pertain only to the X-21 aircraft, at M = 0.75 and 40,000 ft. altitude. For any aircraft, the critical values and the extent of the four regions just discussed are functions of airfoil leading-edge shape and sweep angle, and of aircraft airspeed and altitude. The critical values and extent also depend on the particle shape. All these factors affect the number of ice particles penetrating the boundary layer. One of the goals of the LEFT experiment is to develop, through operational experience, plots such as those of Figure 2 showing the regions for the JetStar aircraft. These may allow a limited validation of the Hall theory developed for the X-21, and allow its extension to other aircraft. Further discussion on these aspects may be found in reference 4.

PREDICTED LAMINAR FLOW DEGRADATION

40 000 ft, M = 0.75, X-21

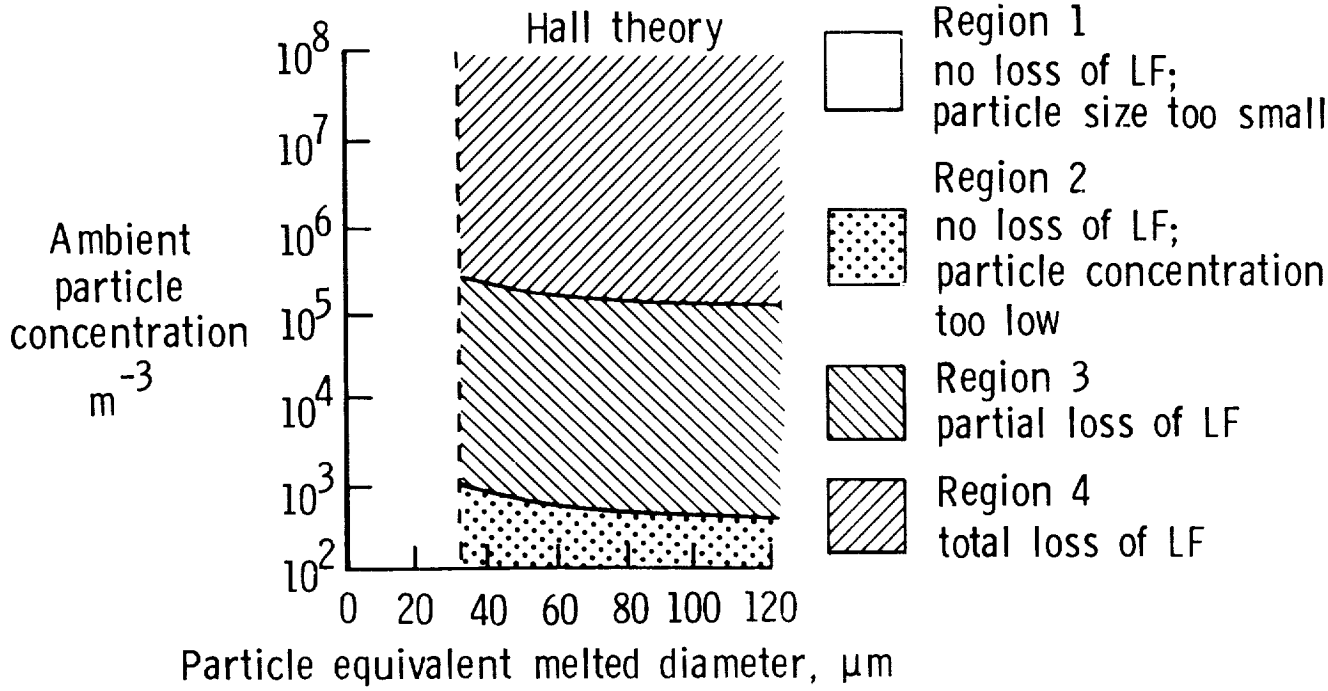

Figure 2

OBJECTIVES OF INVESTIGATION

The objectives of our investigation are summarized in figure 3.

- Evaluate instruments for detecting conditions detrimental to laminar flow (LF)
- Measure cloud/haze particle environment and aircraft charge on all LEFT flights
- Correlate laminar flow extent on both leading-edge test articles with particle environment and aircraft charge
- Analyze data by statistical methods, for significant effects and relationships
- Validate the "Hall criteria", if possible
- Obtain statistical data on the probability of encountering clear air, haze or cloud

Figure 3

CLOUD PARTICLE INSTRUMENTATION ON JETSTAR PYLON

The meteorological instrumentation for measuring the ambient atmospheric particle environment during flights of the JetStar LEFT program consists of two instruments mounted on a pylon extending dorsally from the JetStar fuselage, as shown on Figure 4. The two instruments are a well-proven cloud particle spectrometer, commonly known as a Knollenberg probe, and an experimental particle detector based on a triboelectric (frictional) charge-exchange principle. Both instruments measure the free-stream particle environment, well away from any fuselage-induced concentration effects. A comprehensive description of both instruments may be found in reference 4; an abbreviated description is given next.

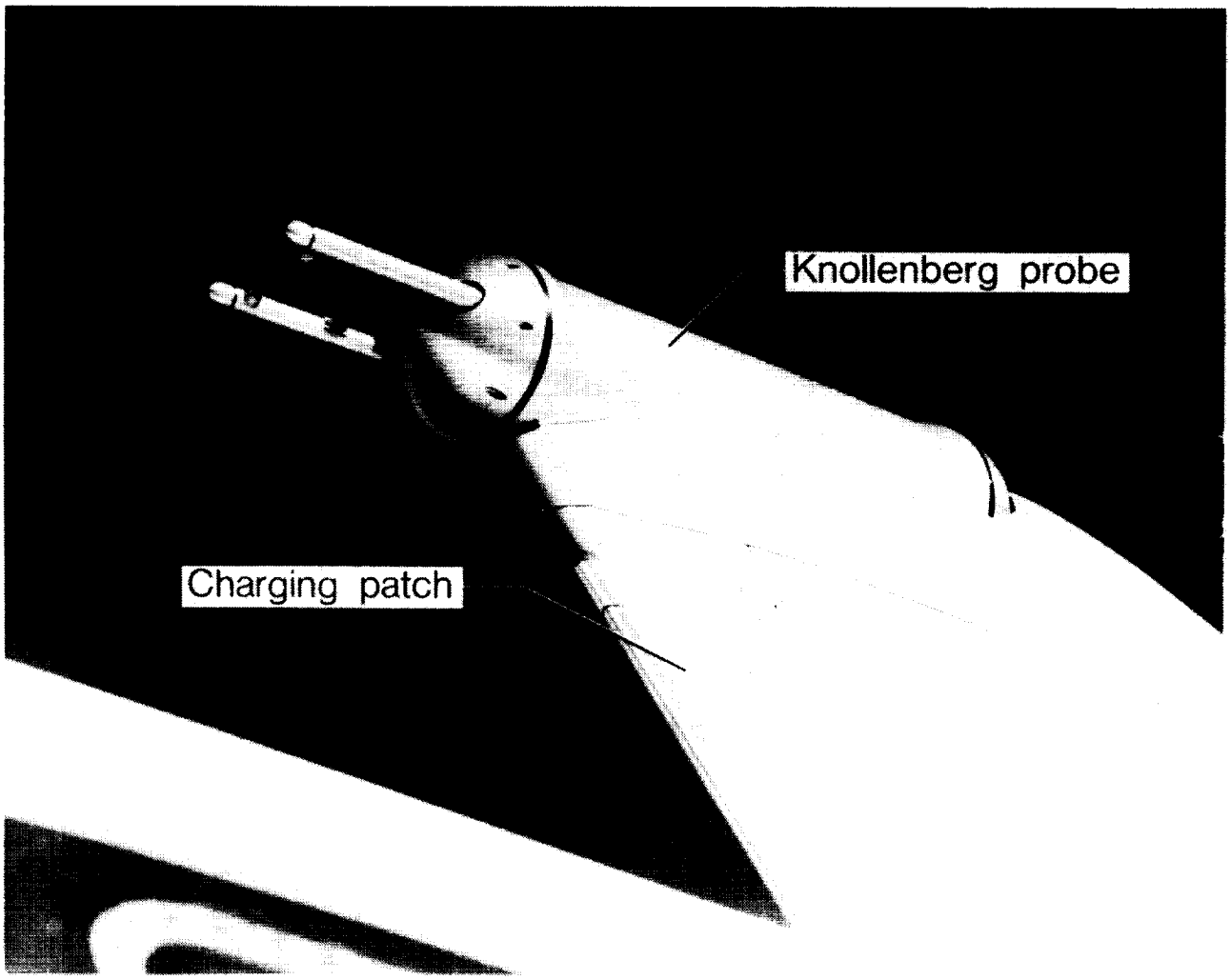

Figure 4

INSTRUMENTATION

CLOUD PARTICLE SPECTROMETER (KNOLLENBERG PROBE)

A Particle Measuring Systems (PMS), Inc. model OAP-230X Optical Array Cloud Droplet Spectrometer Probe; mounted atop the pylon in a cylinder (Fig. 4) is used as a "truth" instrument to measure the spectra (number density versus particle size) of cloud and other particles encountered on the LEFT missions. Figure 5 shows (a) the principle of operation, (b) a diagram of the probe's optical system, and (c) a photograph of the probe in its housing. Part (a) is a snapshot view of a particle passing transversely through the laser beam with the free-stream velocity V_∞. While within the beam, the particle's cross section casts a shadow which is imaged on the elements in the photodiode array. From the number of elements shadowed at any instant, an estimate of the particle's transverse dimension is obtained. The OAP-230X measures particles in 30 size bins between 20 and 600 μm effective size, with a bin resolution of 20 μm. The instrument is designed to provide measurements in all 30 size channels at 100 m sec^{-1} (194 knots) free-stream velocity; because the JetStar flies at approximately 500 kt. (258 m sec^{-1}), however, measurements in the first two size channels, 20-40 and 40-60 μm, are not obtained, but measurements of particles sized between 60 and 600 μm are obtained accurately. From Hall's (ref. 2) analysis, particles larger than 33 μm should affect laminar flow at 40,000 ft. and particles larger than 18 μm should effect laminar flow at 25,000 ft. altitude. Therefore, the probe will provide measurements of most of the particles that are predicted to affect LF, but not all. However, aerodynamic considerations, based on references 5 and 6 suggest that the other instrument (charging patch) is affected by particles down to 20 μm in size. Thus, the readings of both instruments taken together can be used to infer the total particle environment. This suggestion seems to be borne out by our operational experience, in which the charging patch indicates cloud encounters in about 4 percent more cases than does the probe. In most cases, however, both probe and patch indicate particles simultaneously.

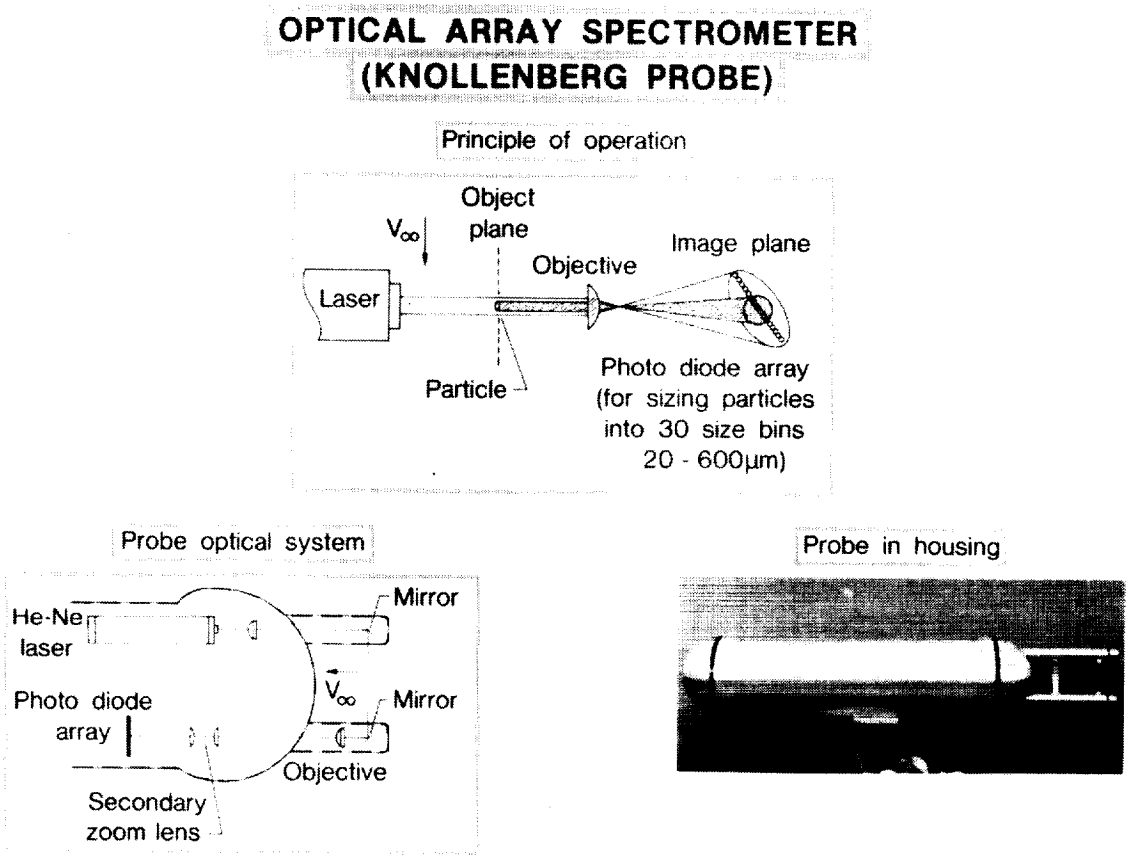

Figure 5

INSTRUMENTATION

CHARGING PATCH

As an aircraft encounters atmospheric particles, whether aerosols, volcanic dust, raindrops or ice crystals, its airframe becomes charged by a triboelectric (frictional) effect. A detailed description of the charging and discharging phenomena associated with aircraft is given in Reference 7. Therein, it is shown that the charge-discharge phenomenon is dependent upon several factors, discussed in the reference. The dependence is complex and cannot be completely described analytically; nevertheless, by electrically isolating part of the airframe as a "charging patch", the level of charging current on the patch may be monitored, and hopefully related to the ambient atmospheric particle environment. The use of charging patches has some precedence, in work in Europe and the USSR, as well as in the USA. Indeed, a charging patch was used on the X-21 aircraft (refs. 1 and 8), where it was found that a charge indication was usually correlated with a loss of laminar flow. NASA-Langley has refined the charging patch concept to the present application, mainly by increasing its sensitivity and using improved fabrication methods (ref. 9). Again, in the JetStar LEFT application, the charging patch is supported by the Knollenberg probe as a truth device. Hopefully through this two-instrument approach, the charging current behavior of this admittedly empirical device can be documented well enough to determine the suitability of the charging patch as a stand-alone cloud particle detector for LFC aircraft application.

METHOD OF CALCULATING THE AREAL PERCENTAGE OF LAMINAR FLOW

As shown in Figure 6 for the port wing, looking aft from the Lockheed test article, an array ("rake") of 20 evenly spaced pitot tubes is mounted behind each leading-edge test article. These near-surface pitot tubes are mounted with their axes about 0.070 inch off the surface. Also, there are 5 stations where two additional probes are installed, at heights from the wing surface of 0.020 to 0.15 inches, and two stations with the pitots about 2.5 inches above the surface. Figure 7 illustrates how the pitot tube readings are used to detect the nature of the boundary layer. The near-surface pitots measure the near-surface total pressure (Pt, probe), and the reference pitots measure the reference pressure ($Pt,_{\infty}$). If laminar flow exists at the pitot tube, the boundary layer will be thin enough to pass under the tube, which will then register a pressure close to the reference pitot. But, if transition occurs ahead of the surface tube, the tube will be immersed in a turbulent boundary layer with much-reduced total pressure, so that (Pt, ∞-Pt, probe) is positive; the value of the pressure differential depends on where (chordwise) the boundary-layer transition occurs. A high pressure differential signifies that transition occurs near the leading edge; a lower value means that transition occurs further along the chord. A correlation of the chordwise location of flow transition and the pressure differential is shown in Figure 8; this correlation is based upon theoretical calculations with an assumed transition location and forced (transition strip) transition measurements. Figure 8 shows the curves used for the Douglas article, and the upper and lower surfaces of the Lockheed article. These curves can only be considered as approximations, and the predicted transition locations are, hence, only approximate at best, Rigorously, the correlation should be a function of several variables (e.g.: altitude, angle of attack, Mach number, span station), but qualitative results should be achievable with these simplified, one curve correlations. (The curves presented are for Mach 0.75 and 36,000 ft. altitude.) On Figure 8, the ratio $\Delta P/q$ is the ordinate, where ΔP is the measured pressure differential and q is the dynamic pressure. The abscissa is $(x/c)_{tr}$, or the fraction of chord at which transition takes place. Both leading-edge test articles extend to about 13 percent chord; the precise values are 0.137 for the Lockheed and 0.129 for the Douglas article.

When the $\Delta P/q$ values for all twenty near-surface pitots are calculated, and allowance is made for the spanwise spacing of the pitots (i.e., area weighting), the total percentage area of the article that is laminar may be estimated; (the estimate is made by summing parallelogram areas as in Figure 9. The figure shows an example from a point in Flight 1059 where it was calculated that 98.63 percent of the area of the Douglas upper article had laminar flow. (The shaded areas in the figure are turbulent.) In this paper, it is the areal percentage of laminar flow, that is analyzed for changes with the ambient cloud particle concentration or charging patch reading.

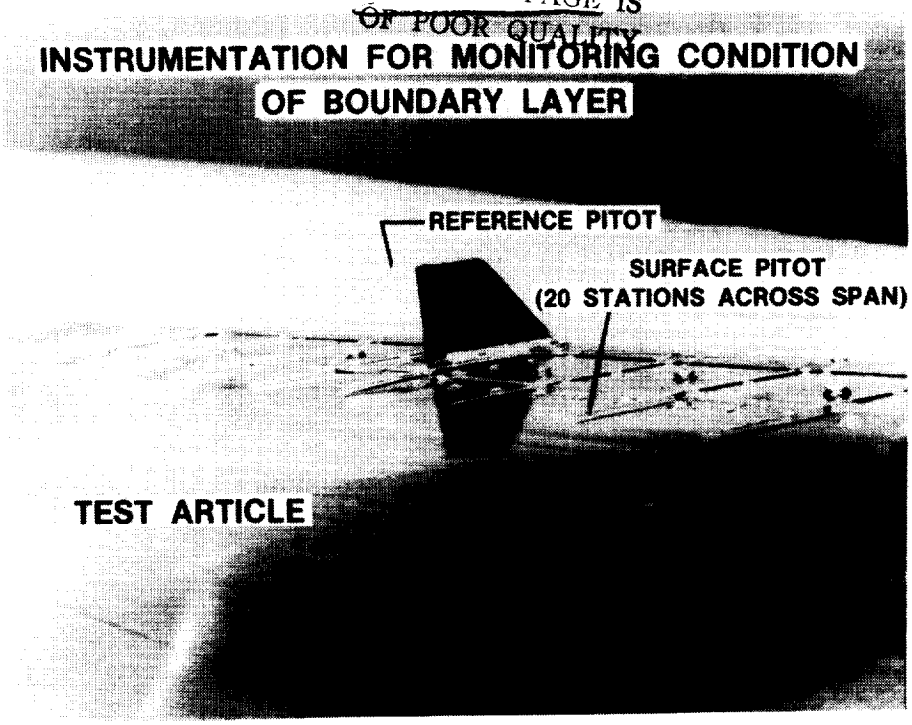

Figure 6

DETERMINATION OF SPANWISE EXTENT OF LAMINAR FLOW AT FRONT SPAR

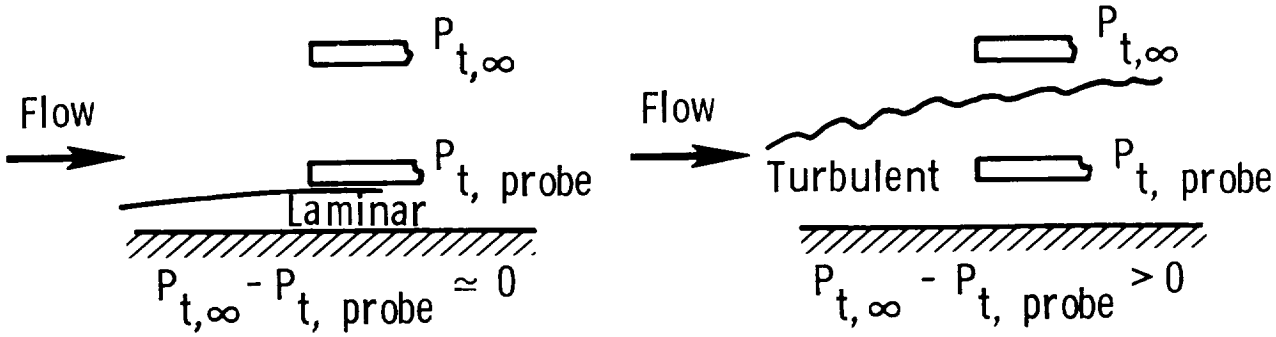

Figure 7

THEORETICAL CHORDWISE EXTENT OF LAMINAR FLOW

M = 0.75, 36000 ft

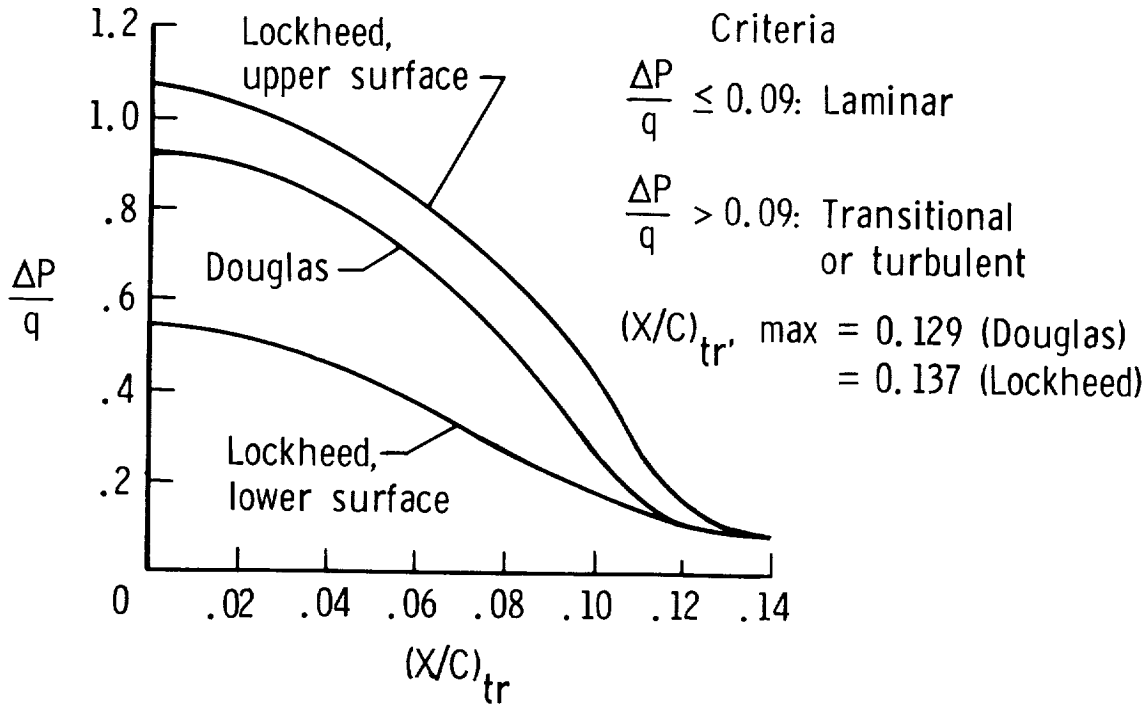

Figure 8

EXAMPLE OF CALCULATION OF AREAL EXTENT OF LAMINAR FLOW

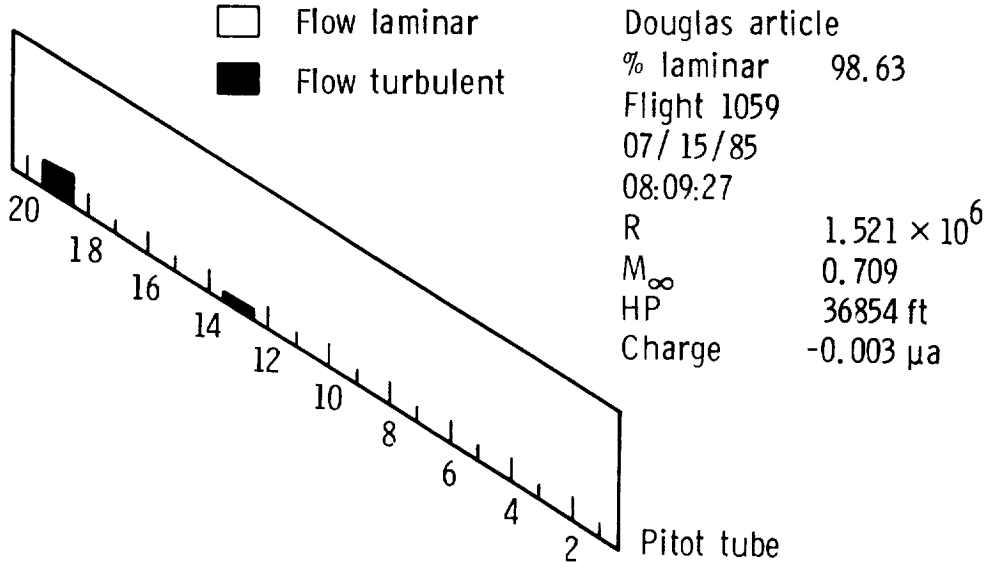

Figure 9

EXAMPLE OF CONCURRENT TRACES OF LAMINAR-FLOW PERCENTAGE AND PARTICLE PROBE AND CHARGING PATCH SIGNALS

Figure 10 shows an example of the concurrent time histories of laminar flow, on the Douglas and Lockheed articles, and of the signals from the particle probe and charging patch instruments. The data are taken from Flight 1099, which was chosen for discussion because it shows a progression from flight in clear air to a cloud encounter, to clear air again. The three panels of the figure show (a) the areal extent of laminar flow on the three test articles, (b) the charging patch current in microamperes (μa), and (c) the total number of particles registered by the particle probe (not the concentration) during each one-second sampling interval. The time traces begin at 9 hrs. 20 min. 00 sec. (0 sec on the figure) and extend 1000 seconds, or to 9 hrs. 36 min. 40 sec. At the beginning of the trace, the Douglas article is indicating 100 percent laminar flow to the front spar, the charging patch current is indicating a "clear air" reading of about -0.04 μa, and the particle count is zero. At about 750 seconds, the percentage of laminar flow decreases precipitously as a cloud element is encountered. An immediate change in the charge level takes place at the same time, and particle counts are noticed, also. This first cloud encounter is temporary, however, and the laminar-flow readings return to near clear air values at about 800 sec. Thereafter, a more sustained encounter with thicker clouds begins at about 830 seconds. Again, the results indicate simultaneous loss of LF, charge current increase, and an increase in the number of particles. The lowest levels of LF are reached at about 860-880 sec. (about 28 percent). At about 945 sec., the aircraft begins to exit the cloud, and charge and particle count are starting to decrease. By about 990 sec., clear air is again encountered.

The degree of LF on all articles changes simultaneously, and the particle count and charging patch readings are related to the degree of laminar flow that is present. The charging patch generally responds slightly before the particle counter does, and the particle counter ceases responding before the charging patch does. This is believed due to the fact that the charging patch responds to a wider range of particle sizes than does the particle counter and is also consistent with expected cloud behavior, with smaller particles and lower particle concentrations surrounding denser concentrations and larger particles. From comparison of the three figure panels, it is also evident that particles smaller than 60 μm definitely affect laminar flow, in addition to those 60 μm and larger in size.

Plots such as these were made for a large number of flights, and statistical analysis was performed, all of which led to the conclusion that both charging patch and particle probe readings can be useful as reliable indicators of the loss of laminar flow.

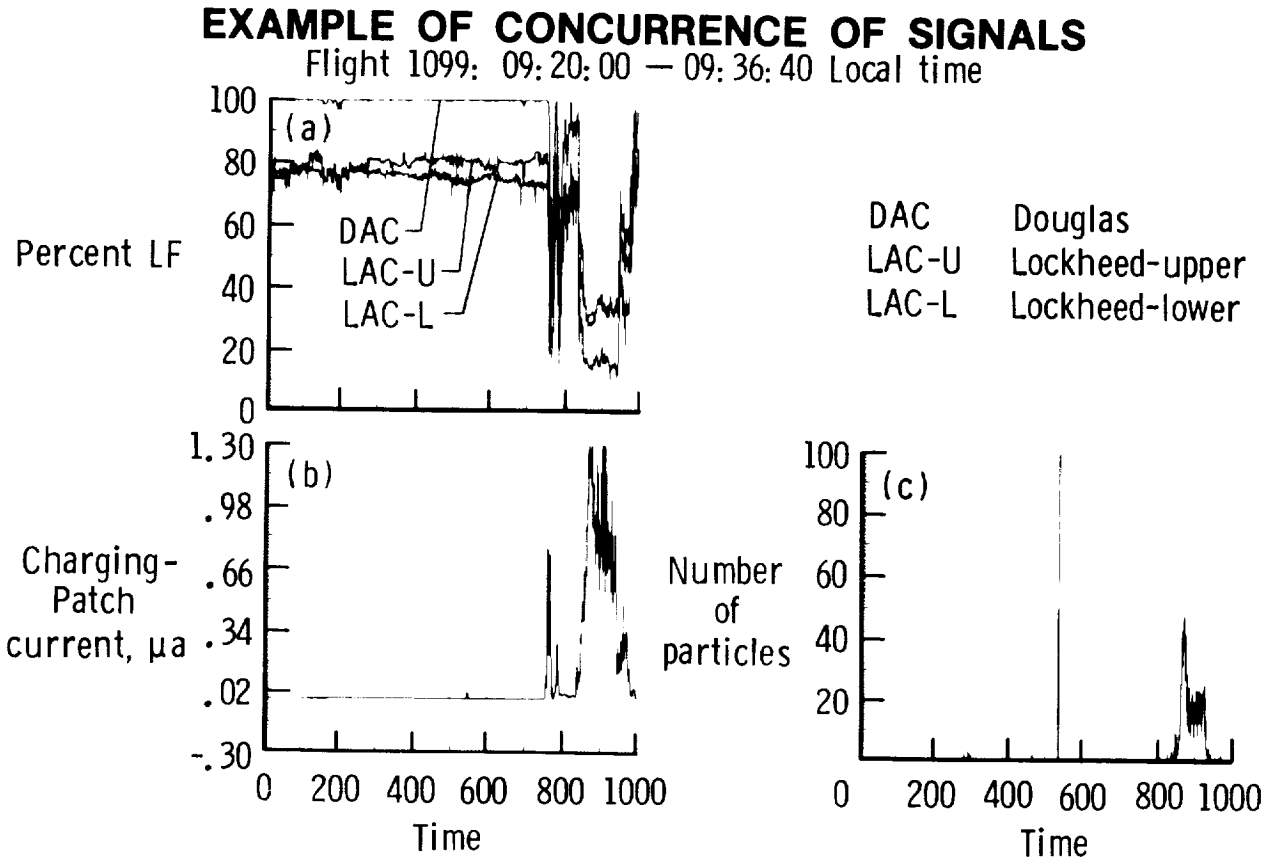
EXAMPLE OF CONCURRENCE OF SIGNALS
Flight 1099: 09:20:00 — 09:36:40 Local time
Percent LF
(a)
DAC
LAC-U
LAC-L
DAC Douglas
LAC-U Lockheed-upper
LAC-L Lockheed-lower
Charging-Patch current, μa
(b)
Number of particles
(c)
Time
Time

Figure 10

SUMMARY OF LAMINAR-FLOW PERFORMANCE AND METEOROLOGICAL ENVIRONMENT ON SIMULATED AIRLINE SERVICE (SAS) FLIGHTS

Figure 11 gives a summary table of the laminar-flow performance and meteorological environment on the 13 Simulated Airline Service (SAS) flights analyzed to date. These particular flights were chosen from the total population of LEFT flights because the data tapes were already in hand, and these flights comprised a range of cloud encounter conditions for thoroughly evaluating the cloud detector instruments. The table lists for each flight: the altitude range, the average percentage of laminar flow (LF) on each article (Douglas, Lockheed upper surface and Lockheed lower surface) during cruise conditions, the cloud environment (percentage of time in clear air, haze, and cloud), the average and maximum values of particle concentration (m^{-3}) derived from the Knollenberg particle spectrometer, and the largest particle measured during the flight, in μm (micro-meters).

For this investigation, "haze" was defined as a total ambient particle concentration of less than 1000 m^{-3}, and "cloud" as an ambient concentration $\geq$ 1000 m^{-3}. "Clear air" is a particle count of zero. (Recall that only particles $\geq$ 60 μm in diameter are measured by the probe). The aircrew notes for missions 1061 and 1104 indicated possible icing on the pitot probes, so some laminar-flow results computed for those missions were not included in the LF analysis. Omitting these two missions, for the 11 SAS flights remaining in the sample, (with 20258 data points) the average LF performance of the Douglas article was 92.32 percent. For the Lockheed article, the average was 73.93 percent for the upper surface, and 69.56 for the lower surface. These average values give little inkling of the dramatic deviations that can occur. For instance, on some missions, the Douglas article indicated about 85 percent while the Lockheed article indicated about 10 percent LF.

As desired, cloud encounter environment varied over the 13 missions chosen for overall analysis. Minimum cloud encounter occurred on Flight 1082, where no particles at all were encountered, yielding a "clear air" figure of 100 percent. Maximum cloud encounter was obtained on Flight 1061 where the JetStar was in cloud for 58.60 percent of the time. The overall percentage of time in clear air, for all 13 missions, is 88.56 percent. The overall percentage for haze is 3.28 and that for clouds is 8.17. This average represents a disproportionate effect of Flight 1061, however, which had a heavy concentration of clouds. That flight represented conditions which undoubtedly would have been avoided (by altitude change, etc.) by the crew of an LFC transport. If Flight 1061 is removed from the sample, the resultant average percentages of time in clear air, haze and cloud for the remaining 12 flights are 92.81, 3.20, and 3.99, respectively, as given in the last line of the table. The combined figure for haze and cloud for the 12 flights is 7.19 percent, which is in good general agreement with our earlier estimate of 6 percent, which was based on an analysis of 1748 flights (6250 hours) of specially instrumented commercial aircraft data (Refs. 10 and 11). The fact that the JetStar number is a little higher is probably related to the fact that the 13 JetStar flights selected for analysis here were chosen because clouds were indeed encountered; in fact, there were several SAS flights where clouds were not encountered at all. Therefore, the figure of 7.19 percent is probably an upper bound on the likelihood of cloud encounter on an overall basis. Overall averages

C-3

for the sample, with data from Flights 1061 and 1104 removed (thus, leaving 11 flights) are included for completeness and for correlation with the overall LFC performance values in the second-to-last row of the table in figure 11.

Cloud particle environments penetrated by the aircraft ranged from the clear air condition of Flight 1082, through the small particle environments of Flights 1087 and 1104 (maximum particle sizes of 180 and 170 m, respectively), through the very thick clouds of Flight 1061, wherein particles up to 600 μm in size were encountered. Average particle concentrations ranged from 0 (Flight 1082) through the thin hazes of Flights 1059, 1060, 1087, and 1103, through the thicker hazes of clouds 1080, 1085, 1094, 1100, and 1104, through the cloud conditions of Flights 1081 and 1099, to the truly thick clouds of Flight 1061, (cf Fig. 11).

It is noted in Figure 11 that the average level of LF on the Douglas article for each flight is close numerically to the percentage clear air value for that flight. Also, the average level of LF is inversely related to the average particle concentration. This apparent agreement was confirmed by regression analysis, where it was found that: $(\%\ LF)_{DAC} = 30.26 + 0.669 \times (\%$ clear air) with a correlation figure of 0.926, for the sample, excluding Flights 1061 and 1104.

LAMINAR FLOW PERFORMANCE AND METEOROLOGICAL ENVIRONMENT
ON THE THIRTEEN SAS+ FLIGHTS ANALYZED

MISSIONS:		LFC PERFORMANCE: $\overline{LF}$ %			CLOUD ENVIRONMENT % TIME IN:			PARTICLE ENVIRONMENT CONC., m^{-3}		SIZE (μm)
FLIGHT	ALTS.(kft)	DAC	LAC UPPER	LAC LOWER	CLEAR AIR	HAZE*	CLOUDS*	AVERAGE	MAX	MAX
1059	32.7-36.9	93.51	83.82	80.25	90.23	5.57	4.21	1.07E2	5.70E3	240
1060	32.7-36.8	93.75	84.59	70.93	94.77	2.90	2.32	1.10E2	1.84E4	300
1061	28.7-32.9	56.47	49.78	**	37.16	4.24	58.60	2.29E5	2.20E6	600
1080	30.7-32.7	91.42	66.01	68.13	91.04	3.82	5.15	2.89E2	2.91E4	440
1081	32.7	89.07	59.03	64.72	94.91	11.29	3.95	8.15E3	3.50E5	600
1082	28.7-32.8	97.96	87.70	79.26	100.00	0.00	0.00	(no particles encountered)		
1085	30.8-32.8	96.74	72.76	70.57	97.55	0.76	1.69	1.97E2	1.69E5	400
1087	26.2-34.7	96.02	79.47	77.34	99.05	0.85	0.10	7.00E1	1.29E5	180
1094	32.5-32.8	86.28	72.61	64.62	84.37	5.89	9.75	3.16E2	8.88E3	440
1099	30.6-34.7	86.24	72.88	65.17	83.51	9.08	7.41	8.66E3	3.60E5	600
1100	22.5-35.7	84.90	51.41	42.78	81.56	8.79	9.64	3.98E2	1.72E4	320
1103	34.7-34.8	97.97	84.95	80.74	99.43	0.28	0.28	1.00E1	3.78E3	200
1104	27.4-34.7	**	**	**	93.78	1.47	4.77	2.57E2	3.03E4	170
* HAZE CONC. < 1.0E3m^{-3}; CLOUD $\geq$ 1.0E3 m^{-3} ** POSSIBLE ICING ON PITOT PROBES										
OVERALL (ALL 13 FLTS.)		———	———	———	88.56	3.28	8.17			
OVERALL (LESS 1061, 1104)		92.32	73.93	69.56	92.69	3.42	3.89			
OVERALL (LESS 1061)		———	———	———	92.81	3.20	3.99			

+Simulated airline service (SAS)

Figure 11

OVERALL PERFORMANCE OF BOTH LEADING-EDGE TEST ARTICLES

Figure 12 presents the overall degree of laminar flow performance for both Douglas and Lockheed leading-edge test articles, obtained in eleven representative SAS (Simulated Airline Service) flights over the altitude range given in Figure 11. A sample of 20258 data points (5.63 hrs. data) was included in the analysis. The results are plotted on probability paper (which accounts for the non-uniform demarcation of the ordinate) and are presented in the form of cumulative probability distributions. All meteorological conditions are included in the sample. (Separate breakouts by clear air, haze and clouds, and by ambient particle concentration are given in subsequent figures). In explanation, the ordinate gives the probability, in percent, that the extent of laminar flow on the article (i.e. back to the front spar) equals or exceeds the abscissa value. Three curves are given, one for the Douglas article, and one each for the upper and lower wing leading-edge surfaces of the Lockheed article. In an example, it is seen from the figure that the probability that the degree of laminar flow on the Douglas article equals or exceeds 30 percent is about 98 percent. Similarly, the probability of achieving or exceeding 70 percent ($P \geq 70\%$) is about 89 percent, $P(\geq 90\%)$ = 84 percent, $P(\geq 95\%)$ = 82 percent and $P(\geq 99\%)$ = 63 percent. It may be inferred that the probability of achieving less than 30 percent LF was less than 2 percent; this means that this article was almost always (98 percent of the time) experiencing a degree of LF $\geq$ 30 percent.

Similar deductions can be made from the cumulative frequency plots for the Lockheed upper and lower surfaces. The Lockheed upper surface experienced at least 30 percent LF 96 percent of the time, but achieved $\geq$ 99 percent only about 2.5 percent of the time (versus 63 percent of the time, for the Douglas article). For the lower surface of the Lockheed article, the probability of exceeding a given degree of laminar flow is somewhat less than that for the upper surface, because of the more adverse chordwise pressure gradient on the lower surface.

To provide additional information, the average values of LF for the 20258 data point ensemble are plotted as solid symbols on the figure. The average values are 92.3 percent for the Douglas article, 74 percent for the upper surface of the Lockheed article and 70 percent for the Lower surface of the Lockheed article. An arrow is placed on the ordinate to denote the median (50th percentile) point. Reading across from this point, the median values are: Douglas article > 99 percent; Lockheed upper > 80 percent; Lockheed lower > 74.5 percent.

Another depiction of the same data is given as Figure 13, which is a histogram plot of the percentage of cases with a given degree of LF. For example, in the band with > 99 percent LF, it is again seen that about 63 percent of the cases for the Douglas article lay in this category, versus only about 2.5 percent for the Lockheed article, both for its upper and lower surfaces.

Finally, it should be mentioned that 92.7 percent of the cases in this 11-flight data sample were obtained in clear air, 3.4 percent in haze, and 3.9 percent in cloud.

EXTENT OF LAMINAR FLOW ON TEST ARTICLES IN ELEVEN FLIGHTS IN SIMULATED AIRLINE SERVICE

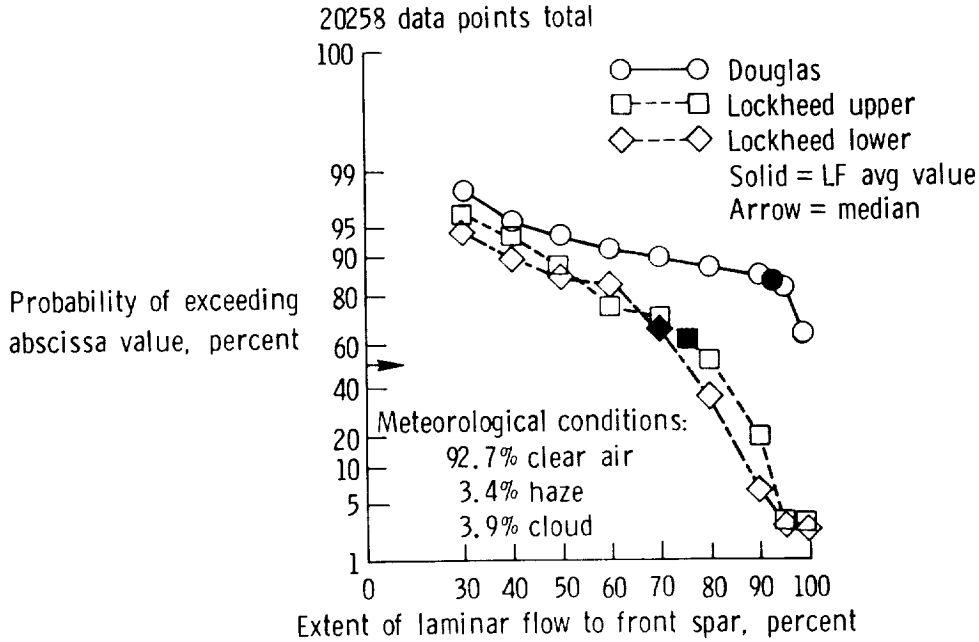

Figure 12

HISTOGRAM PLOT: DISTRIBUTION OF LF OBSERVATIONS OBTAINED IN ELEVEN SIMULATED AIRLINE SERVICE MISSIONS

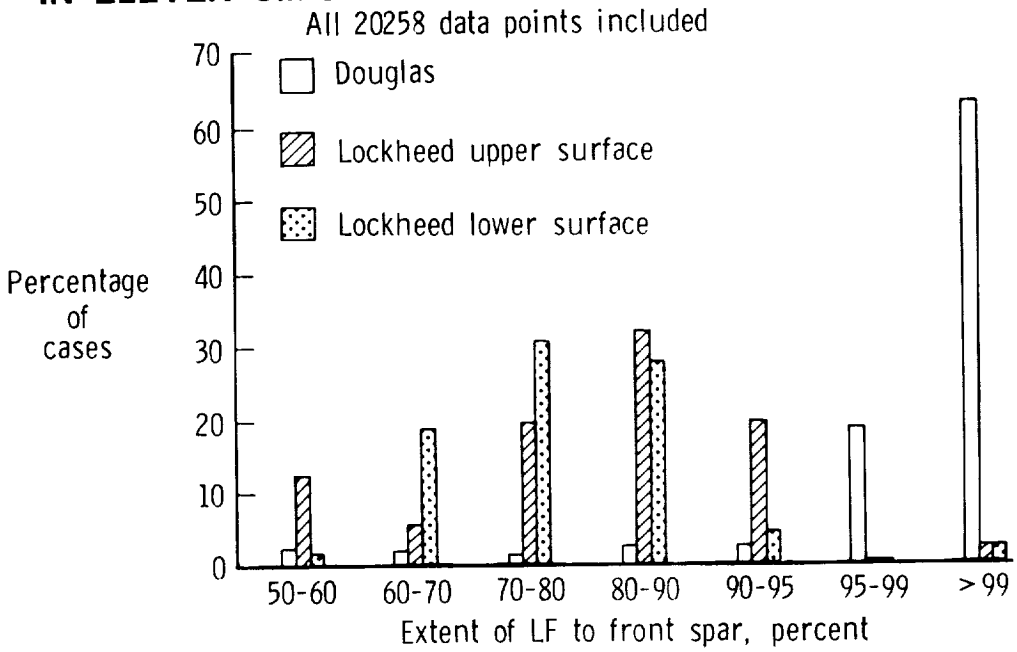

Figure 13

PERFORMANCE OF DOUGLAS ARTICLE IN CLEAR AIR, HAZE, AND CLOUDS

Figure 14 presents a series of cumulative probability distribution plots describing the LF performance of the Douglas leading-edge test article in clear air, haze, and clouds separately, as well as overall. (The overall plot is the same as that presented on Figure 12). For this investigation, "clear air" is arbitrarily defined as a total ambient particle concentration of 0, as measured by the Knollenberg probe particle spectrometer. "Haze" is defined as a non-zero total concentration of $< 1000\ m^{-3}$, and "cloud" as an ambient concentration $\geq 1000\ m^{-3}$. Only plots for the Douglas article are presented, because only that article showed a high probability of achieving a high level of laminar flow, in clear air conditions. (This is felt to be the result of surface imperfections in the Lockheed article, rather than to any intrinsic lack of merit of the slotted [versus porous] concept).

The results for clear air show that there is a 98.8 percent probability of achieving at least 30 percent LF, a 91 percent probability of $\geq$ 90 percent LF and a 78 percent probability of achieving $\geq$ 99 percent LF.

The results for haze show a marked decrease in probability of achieving a given degree of LF, compared to that in clear air. The results in cloud show a further marked decrease. Both decreases were found to be statistically significant. Thus, the X-21 experience is verified on statistical grounds, for the first time. The cumulative probability values for comparison to the clear air values stated above are, for haze: $P(\geq 30\%) = 96\ \%$, $P(\geq 90\%) = 13\%$, and $P(\geq 99\%) = 6.2\%$. For cloud, the values are: $P(\geq 30\%) = 78\%$, $P(\geq 90\%) = 6\%$, $P(\geq 99\%) = 5.8\%$. The overall plot is nearer the clear air plot than to any of the other curves; this merely reflects the fact that the preponderance of observations was obtained in clear air conditions.

Just as on figure 12, the average values of LF have been plotted as solid symbols. The average value is 96.3 percent for clear air, 62.5 percent in haze, and 45.2 percent in cloud. The overall value, 92.3 percent, is the same as that shown on figure 12. The median values are 99 percent in clear air, 61 percent in haze and 38.2 percent in cloud.

From the above results, there can remain no doubt that encounter with haze and cloud conditions causes a significant effect on the degree of LF performance of the Douglas article. The results for the Lockheed article, not presented here, show a similar marked effect.

EXTENT OF LAMINAR FLOW ON DOUGLAS TEST ARTICLE, DURING ELEVEN FLIGHTS IN SIMULATED AIRLINE SERVICE

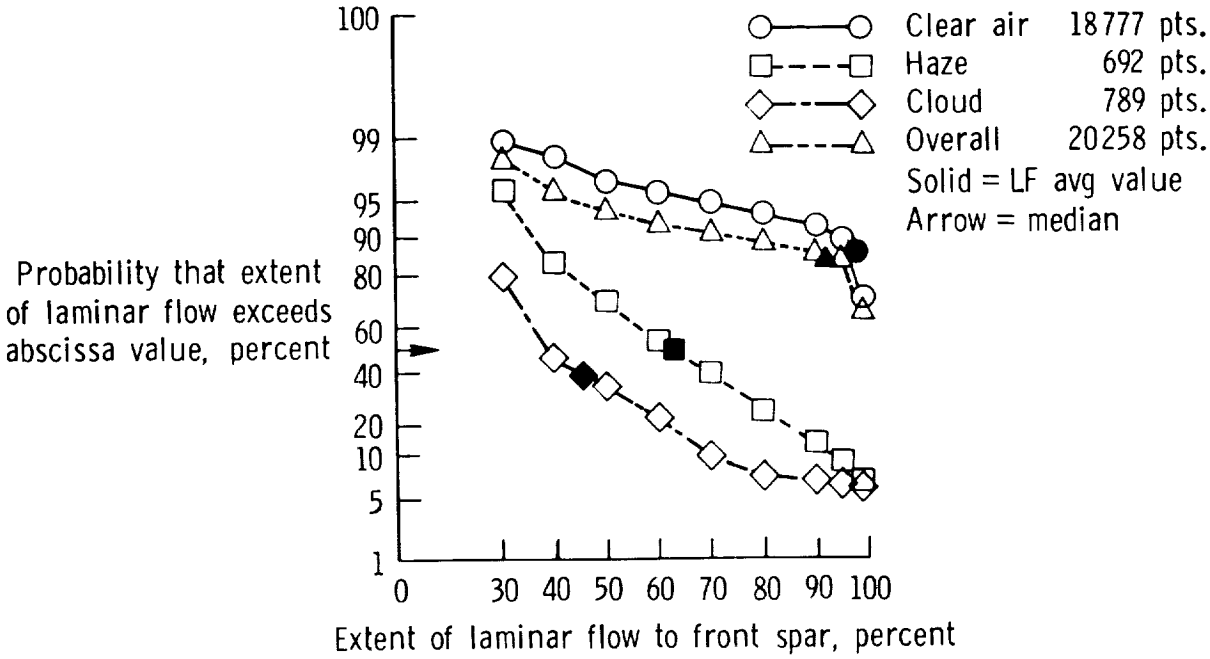

Figure 14

PERFORMANCE OF DOUGLAS ARTICLE IN VARIOUS LEVELS
OF TOTAL PARTICLE CONCENTRATION

Figure 15 is another series of cumulative probability distribution plots. This time, a separate plot is presented for each range of total particle concentration in m^{-3}. The plot for zero concentration is the clear air plot from figure 14, and the overall plot is also common to that on figures 12 and 14.

A marked decrease in the probability of exceeding a given extent of laminar flow is observed, when the ambient concentration increases from zero to a thin haze value of 100-250 m^{-3}. As particle concentration increases further to thicker hazes, a continued decrease in probability is observed. As cloud level concentrations are achieved ($\geq$1000 m^{-3}), the degree of probability decrease is hastened. The curves presented here account for 99 percent of all the data. At still higher concentrations occurring in the remaining one percent of cases, the data (not presented here for the sake of clarity) show that further decreases occur. As before, solid symbols denote the average values of LF-in this case, average values for each level of total particle concentration.

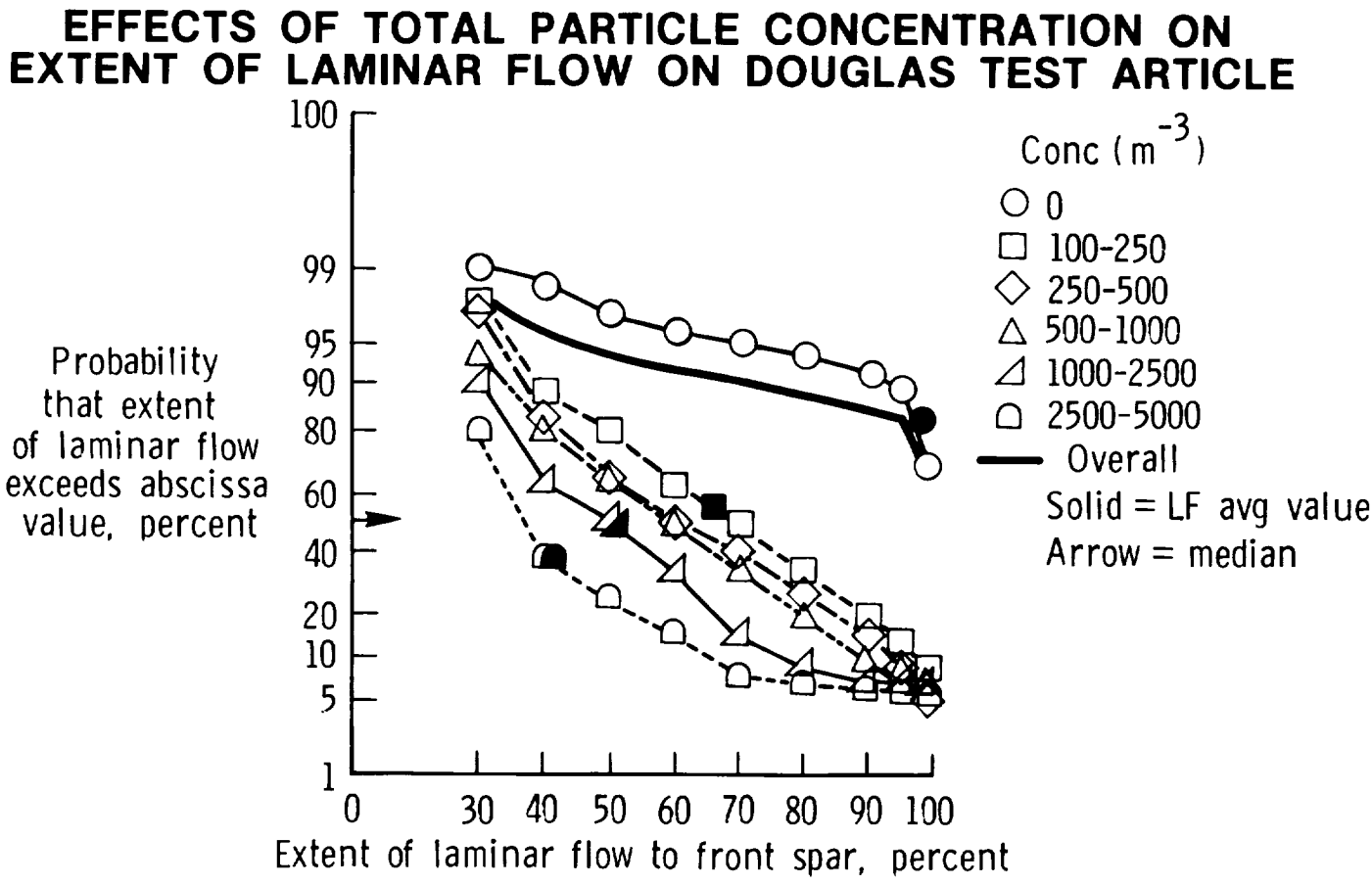

Figure 15

VALIDATION OF HALL CRITERIA WITH JETSTAR DATA

As previously mentioned, one of the goals of our investigation was to attempt to validate the Hall criteria, originally developed to explain LF loss on the X-21 aircraft, with data from the LEFT program. The Hall criteria were presented earlier (Fig. 2). Figure 16, presented below, is a copy of the Hall criteria in Figure 2, overlaid with observations of particle concentrations and values of the concurrent degree of LF loss, computed as described earlier, for Flight 1061, where many clouds were encountered, with a large range of particle concentrations. Particle concentrations computed from Knollenberg probe data were plotted for laminar-flow values lying in three arbitrarily chosen distinct ranges of LF on the Douglas article: 25-35 percent, 75-85 percent, and greater than 85 percent. Several distinct sampling times were chosen at random for each of these ranges, so that 30 times were chosen, overall.

From study of figure 16, it is evident that the range of concentrations corresponding to the 25-35 percent LF range is considerably higher than that for the 75-85 percent range. The range 85-100% had, for the most part, no particles at all observed, so the preponderance of observations lay at the bottom of the figure, within Hall region 2 of fig. 2 where it is predicted that LF will not be lost. However, there were some observations of high LF lying in Hall region 3 (of Fig. 2), which is the region of partial LF loss. These observations are believed consistent, however, with the fact that a high but not 100% reading of LF over the leading-edge test article is very probably associated with a lower overall chordwise percentage of LF.

As cautioned earlier, only a limited degree of validation of the Hall criteria may be possible, because airfoil shape, altitude, and Mach number conditions are different from those for which the Hall figure was derived. JetStar LF is measured to only about 13 percent, rather than full-chord. Nevertheless, the data do seem to show "Hall criteria-like" behavior, in that increasing particle concentrations do lead to progressively smaller degrees of laminar flow. Therefore, it is concluded that the Hall criteria seem to be consistent with JetStar observations, and that the criteria are validated qualitatively.

EXAMPLE OF VALIDATION OF "HALL CRITERIA"

Flight 1061

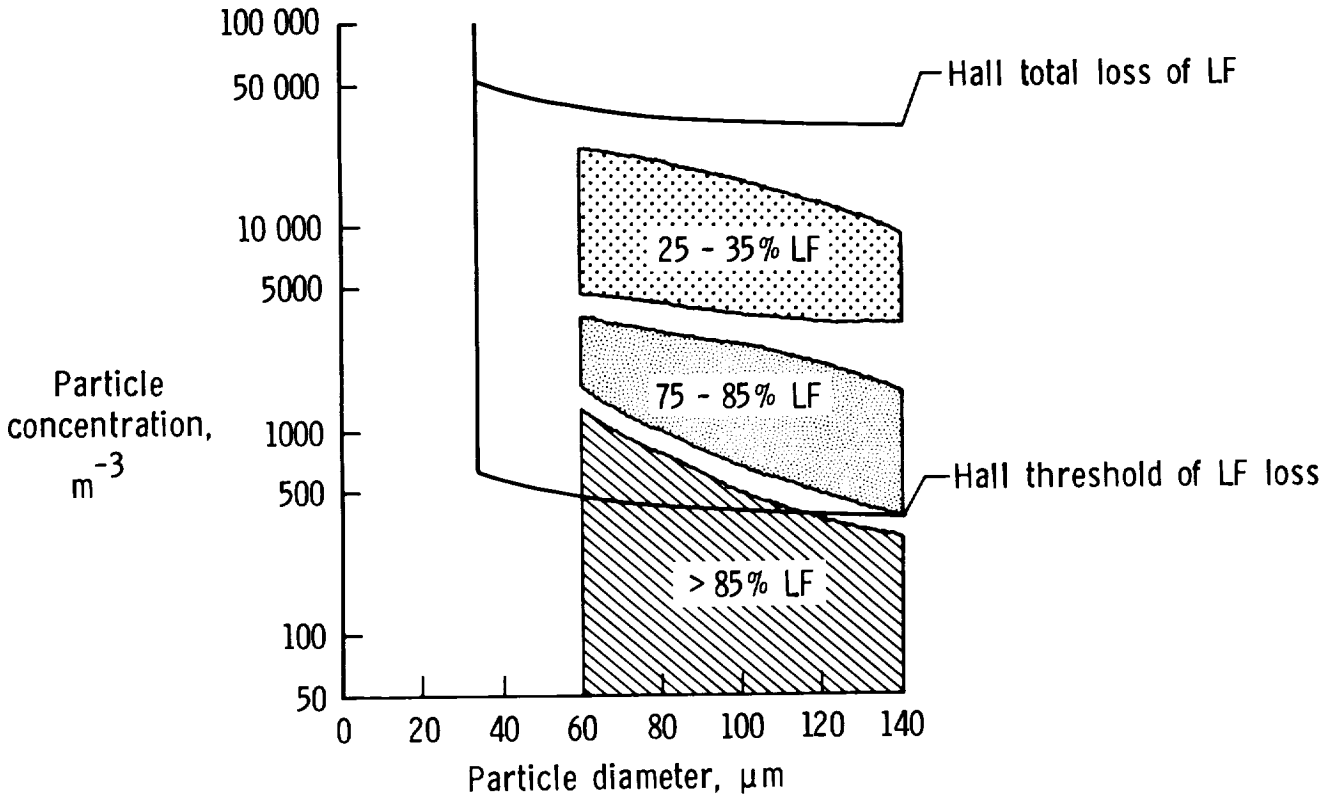

Figure 16

PROBABILITY OF ENCOUNTERING VARIOUS PARTICLE CONCENTRATIONS

Figure 17 is another cumulative probability distribution, which shows the probability of obtaining a total ambient particle concentration which equals or exceeds the abscissa value. The solid curve represents the distribution from 12 SAS missions with 22837 data points. Data from Flight 1061 was not included in this curve, because the percentage of time in cloud on that flight was very high (58.60 percent) and represented a condition which undoubtedly would have been avoided by the aircrew of an LFC transport by using flight management procedures (change of altitude or rerouting). All the other flights constituted conditions into which an LFC aircraft would conceivably have been flown. Nevertheless, for completeness, results with Flight 1061 included are also presented on the figure, as the dashed curve.

Viewing the solid curve results, it is seen that an ambient particle concentration of 100 m^{-3} is attained or exceeded in only about 7 percent of cases. Clouds (concentration $\geq$ 1000 m^{-3}) were encountered on only about 4 percent of cases. From this plot, it might be inferred that the aircraft encountered essentially clear air conditions some (100 -7) or 93 percent of the time. This figure is consistent with earlier estimate of about 6 percent, obtained both in the X-21 project (ref. 1) and in our earlier empirical estimates, based on the analysis of GASP data (ref. 11). Also, the 93 percent figure is very close to the average amount of LF on the Douglas article, shown to be 92.32 percent. From this comparison, it might be inferred, as a general rule, that the average level of LF experienced on a flight is equal to the percentage of time spent in "clear-air" on the flight, for a well-performing test article.

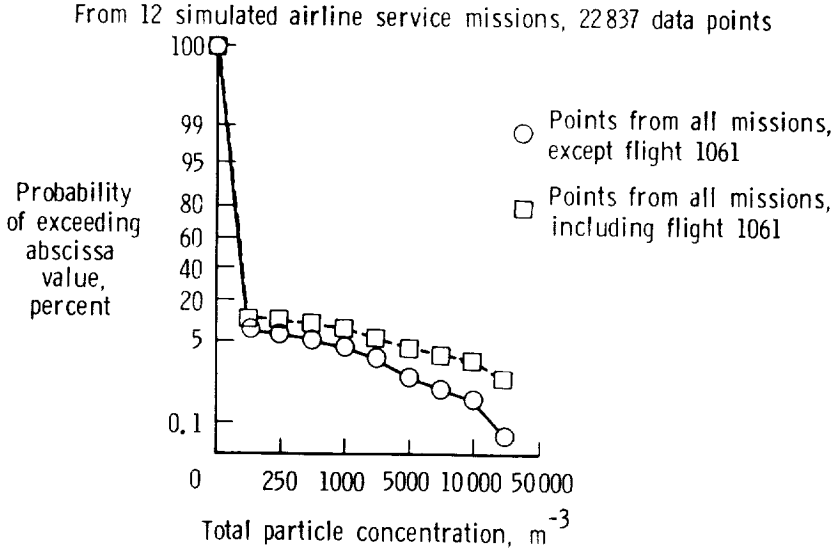

Figure 17

PHOTOGRAPHS OF HAZE CONDITIONS, WITH VARIOUS DEGREES OF LF LOSS

The need for onboard instrumentation for discerning the presence of ambient particle concentrations is sometimes questioned. True cloud conditions are, of course, visible in daylight, but the presence of haze may be difficult to discern, particularly if observer-Sun angles are unfavorable. Also, it is frequently difficult to assess ambient haze and cloud conditions at night. As an example of questionable haze conditions, figure 18 shows two photographs from Flight 1099 (this flight was discussed previously in connection with Figure 10). Both pictures were taken by the JetStar aircrew, while looking out of the port side of the aircraft, with the Sun behind the camera; the port wing is apparent in each photograph. A "haze" condition is apparent at about the elevation level of the wingtip. Photo A was taken at 9:24:00 local time (corresponding to the 240-second mark on Figure 10). Photo B was taken at 9:33:00 (corresponding to the 780-second mark on Figure 10).

When the first photograph (panel a) was taken, the Douglas article was indicating 100 percent LF. During the second photograph (panel b) the degree of LF was 80 percent. Yet, the difference in haze conditions between the two photographs is not very apparent. For conditions such as these, an instrument which indicates the presence of cloud or haze particles would be most useful.

9:24:00 local time, 100% LF

(A)

Figure 18

HAZE CONDITIONS ON FLIGHT 1099

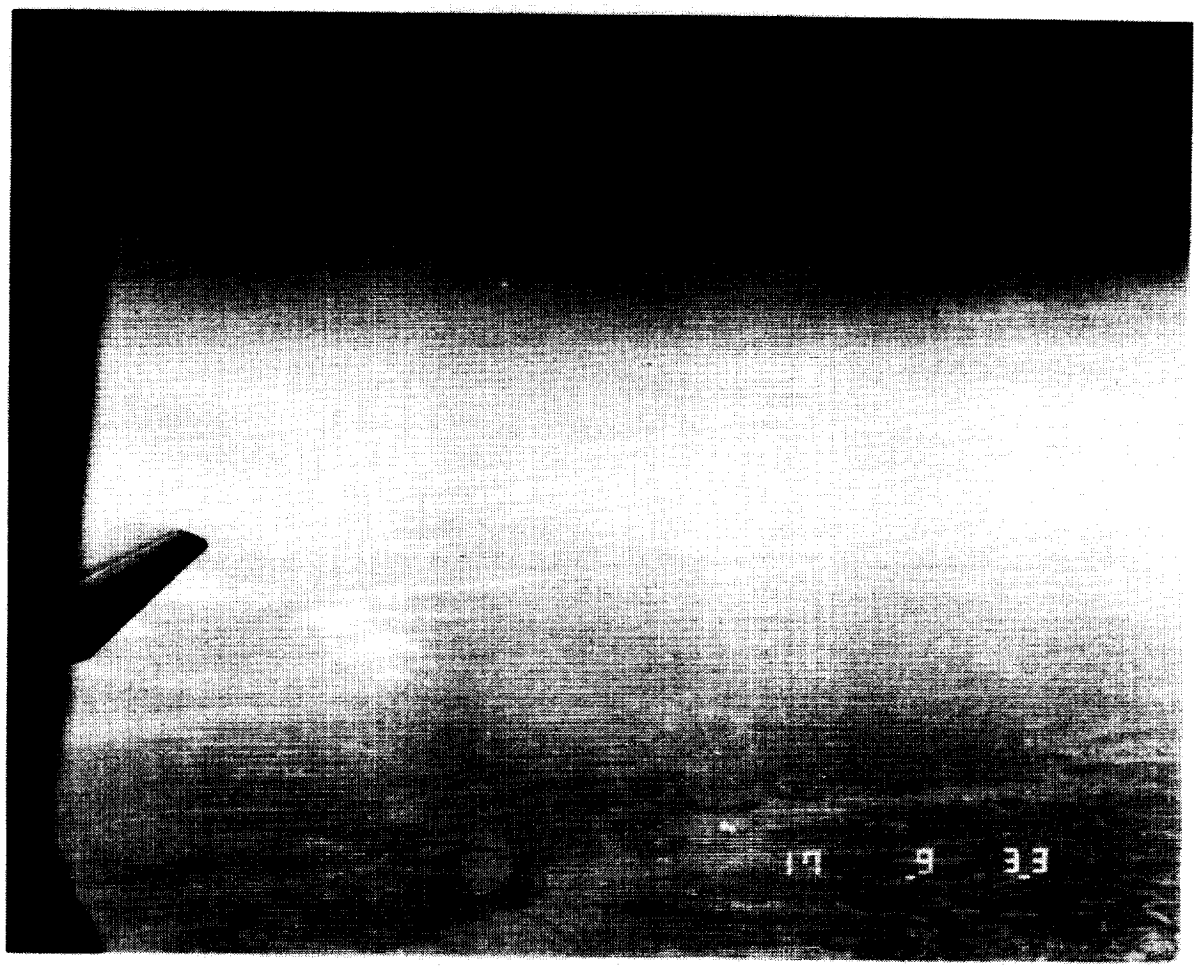

(B)

Figure 18

COMPARISON OF PARTICLE PROBE AND CHARGING PATCH AS DIAGNOSTIC INSTRUMENTS FOR LFC AIRCRAFT

The table shown in Figure 19 presents a comparison of the performance of the Knollenberg probe particle spectrometer and the charging patch for detecting conditions favorable or unfavorable to the maintenance of laminar flow. The evaluation is based on the sample of eleven simulated airline service flights discussed previously (20258 data points).

A two-level reading approach was adopted for simplicity. For the probe, the levels are (1) a total particle count of zero, presumably related to a clear air condition in the ambient, and (2) a non-zero particle count, obviously related to the presence of clouds, haze, etc. For the charging patch, the two levels are: (1) a "zero-range", chosen empirically to be associated with a minimum particle count reading from the probe, and (2) a "non-zero" range, comprising readings outside the zero range. The zero range was determined to be from -0.05 to 0.00 μa (microamperes).

In an example use of the table, a particle probe reading of zero is associated with a $\geq$ 90 percent extent of laminar flow on the Douglas article 90.36 percent of the time. If the particle probe reading is non-zero, there is only a 9.72 percent chance of there being $\geq$ 90 percent laminar flow. Thus, the two levels discriminate effectively between LF-favorable and LF-unfavorable conditions.

Continuing the same example, if the charging patch is used as the diagnostic instrument, a "zero-range" reading is associated with a $\geq$ 90 percent level of LF 92.74 percent of the time. A non zero-range reading is associated with this level of LF only 21.99 percent of the time. Thus, an effective discrimination is again made.

In performing a series of comparisons in this way, it is seen that the two devices give comparable performance, with the charging patch giving slightly more reliable indications of clear air conditions, and the particle probe giving more reliable indications of conditions for loss of LF. This is explained easily by noting that the particle probe is sensitive only to particles 60 μm and larger in diameter, whereas the patch responds to smaller particles as well. These smaller particles do, however, also affect LF, so it is not surprising that a zero-range reading is a better indicator of LF-favorable conditions than is a zero particle count reading. In un-clear conditions, the results are reversed. The reason for this is that a non-zero particle probe reading is indeed associated with the presence of larger particles which more effectively degrade LF than do the smaller ones, whereas a non-zero charge patch reading may result, in part, from the more numerous smaller particles which do not have as marked an impact on LF. Therefore, the non-zero range probabilities of achieving a given level of LF are somewhat larger than those for the non-zero probe probabilities, at the same level of LF. Nevertheless, the non-zero range patch probabilities are still low enough to indicate that the two-level charging patch device provides an effective discrimination between LF-favorable and LF-unfavorable conditions. For this reason, the patch is favored over the particle probe, due to its low cost and simplicity.

COMPARISON OF PARTICLE PROBE AND CHARGING PATCH AS DIAGNOSTIC INSTRUMENTS FOR LFC AIRCRAFT

PROBABILITY OF ACHIEVING DESIRED EXTENT OF LAMINAR FLOW ON DOUGLAS ARTICLE, PERCENT

DESIRED EXTENT OF LAMINAR FLOW, PERCENT	PARTICLE PROBE READING		CHARGING PATCH READING	
	0	≠0	IN "ZERO RANGE"*	NOT IN "ZERO-RANGE"
≥30	98.90	86.50	98.88	91.77
≥40	98.28	62.39	98.52	74.55
≥50	96.85	50.00	97.40	63.40
≥60	95.48	35.79	96.39	51.29
≥70	94.27	23.43	95.54	40.35
≥80	92.93	15.06	94.47	32.67
≥90	90.36	9.72	92.74	21.99
≥95	87.76	7.78	91.01	13.21
≥99	67.55	6.14	70.60	5.99

*"ZERO-RANGE = -0.05 → 0.00 μA

NOTES: 1. 20258 DATA POINTS IN SAMPLE, FROM 11 SAS FLIGHTS
2. PARTICLE PROBE COUNTS PARTICLES 60 μM DIAMETER AND LARGER

Figure 19

CONCLUDING REMARKS

Conclusions and summary comments regarding our investigation of the thirteen JetStar simulated airline service flights so far analyzed are given in figure 20.

LEFT program results

- An extensive data bank of concurrent measurements of laminar flow (LF), particle concentration, and aircraft charging state has been gathered for the first time.
- From this data bank, 13 flights in the simulated airline service (SAS) portion have been analyzed to date. A total of 6.86 hours of data at one-second resolution have thereby been analyzed.
- An extensive statistical analysis, for both leading-edge test articles, shows that there is a significant effect of cloud and haze particles on the extent of laminar flow obtained.
- ~ 93 percent of data points simulating LFC flight were obtained in clear air conditions; ~ 7 percent were obtained in cloud and haze. These percentages are consistent with earlier USAF and NASA estimates and results.
- The "Hall" laminar flow loss criteria have been verified qualitatively.
- Larger particles and higher particle concentrations have a more marked effect on LF than do small particles.
- A particle spectrometer or a charging patch are both acceptable as diagnostic indicators of the presence of particles detrimental to laminar flow.

Figure 20

avg	average
conc.	concentration
DAC	Douglas Aircraft Company
EMD	Equivalent Melted Diameter (of ice particle)
GASP	Global Atmospheric Sampling Program
HP	pressure altitude
LAC	Lockheed Aircraft Corporation
LAC-L	lower surface of Lockheed article
LAC-U	upper surface of Lockheed article
L.E.	Leading Edge
LEFT	Leading-Edge Flight Test
LF	Laminar Flow
LFC	Laminar-Flow Control
M	free-stream Mach number
P ( )	probability of ( )
PMS	Particle Measuring Systems, Inc.
Pt, probe	total pressure, measured at near-surface pitot probe
Pt,∞	free-stream total pressure
q	dynamic pressure
R	Reynolds number
SAS	Simulated Airline Service
V_∞	free-stream velocity
ΔP	measured pressure differential
μa	microampere = 1×10^{-6} ampere
μm	micrometer = 1×10^{-6} m

REFERENCES

1. Whites, R. C.; Sudderth, R. W.; and Wheldan, W. G.: Laminar Flow Control on the X-21. Astronautics and Aeronautics, (AIAA), Vol. 4, No. 7, July 1966.

2. Hall, G. R.: On the Mechanics of Transition Produced by Particles Passing Through an Initially Laminar Boundary Layer and the Estimated Effect on the LFC Performance of the X-21 Aircraft. Northrop Corp., October 1964.

3. Pfenninger, W: Design Considerations of Long-Range and Endurance LFC Airplanes with Practically All Laminar Flow. NASA Joint Institute for Advancement of Flight Sciences. Aug. 1982.

4. Davis, R. E.; and Fischer, M. C.: Cloud Particle Effects on Laminar Flow in the NASA LEFT Program: Preliminary Results. AIAA Paper 86-9811, 1986.

5. Dorsch, R. G.; Brun, R. J.; and Gregg, J. L.: Impingement of Water Droplets on an Ellipsoid With Fineness Ratio 5 in Axisymmetric Flow. NACA TN 3099, March 1954.

6. Brun, R. J.; and Dorsch, R. G.: Impingement of Water Droplets on an Ellipsoid With Fineness Ratio 10 in Axisymmetric Flow. NACA TN 3147, May 1954.

7. Imyanitov, I. M.: Aircraft Electrification in Clouds and Precipitation. (Edited Translation of "Elektrizatsiya Samoletov v Oblakakh Osadkakh", 1970, pp. 1-211). Report FTD-HC23-544-70, U.S. Air Force, April 1971.

8. Mee, T. R.: An Investigation of Atmospheric Factors that May Affect Laminar Flow Control. Report MRI-64-R212A, Meteorology Research, Inc. Altadena, California, December 1964.

9. Campbell, R. E.; and McPherson, J. P.: Cloud Particle Detector. NASA Tech Brief LAR 13137, 1983.

10. Jasperson, W. H.; Nastrom, G. D.; Davis, R. E.; and Holdeman, J. D.: GASP Cloud-and Particle Encounter Statistics, and Their Application to LFC Aircraft Studies (2 vols.). NASA TM 85835, October 1984.

11. Jasperson, W. H.; Nastrom, G. D.; Davis, R. E.; and Holdeman, J. D.: GASP Cloud Encounter Statistics: Implications for Laminar Flow Control Flight. J. of Aircraft, Vol. 21, No. 11, November 1984, pp. 851-857.